

H. Rehage  
B. Achenbach  
M. Geest  
H. Wilhelm Siesler

## Ultrathin dynamic networks formed by the surfactant SPAN 65 at the air–water and oil–water interface

Received: 23 October 2000  
Accepted: 3 November 2000

H. Rehage (✉) · B. Achenbach · M. Geest  
Institut für Physikalische Chemie  
Universität Essen  
45117 Essen, Germany  
e-mail:heinz.rehage@uni-essen.de  
Tel.: +49-201-1833987  
Fax: +49-201-1833951

H. W. Siesler  
Institut für Physikalische  
und Theoretische Chemie  
Universität Essen  
45117 Essen, Germany

**Abstract** Some surfactants tend to form ultrathin films at the surface of water or at the interface between oil and water. A representative of these surface-active compounds is SPAN 65 (trioctadecanyl ester of sorbic acid). Induced by attractive interactions these molecules can self-associate to form temporary networks. At the planar surface we measured the two-dimensional relaxation modulus, the storage modulus, the loss modulus and the relaxation spectrum. In addition to these measurements, we have also investigated the molecular structure

of these networks with “Brewster-angle-microscopy”. The results indicate that temporary cross-linking points, which have lifetimes of the order of a few seconds, tend to stabilize these films. This dynamic network formation is also interesting for numerous technical applications, and it might be used for the preparation of emulsions, foams or microcapsules.

**Key words** Surface viscosity · Surfactant · Surface elasticity · Brewster-angle microscopy

### Introduction

Liquid interfaces between different polar phases play an important role for numerous applications in industry and science. Films formed by conventional surfactants tend to be in a liquid-analogous state and these structures are therefore sensitive to mechanical stresses. Viscoelastic films prepared at the interface by cross-linking processes are more stable. Owing to these properties such ultrathin membranes are often used as model systems for biological cell membranes, which are more complicated owing to their complex structures [1]. Besides the formation of liquid-analogous films, some surfactant can also form gel-like structures. This is a natural consequence of strong attractive forces between the surface-active compounds. In general, such interactions lead to the appearance of viscoelastic effects and unusual film properties.

It is well known, that the surfactant SPAN 65, trioctadecanyl ester of sorbic acid, tends to form very stable emulsions. On the grounds of these special

features, this surface-active compound is frequently used in technical applications. Typical examples of these technologies include the formation of foams, microcapsules or concentrated emulsions. It is well known that the stability of these disperse systems depends very much on the rheological properties of the surfactant films [2]. Enhanced emulsion stabilities are often correlated with large values of the surface viscosity or elasticity [3]. The principal condition of forming highly viscous, gel-like superstructures lies in the tendency of the surfactant molecules to arrange themselves into long chains, which are connected and interwoven. Any two-dimensional network must meet the condition of coherence: this means that the basic elements are joined to form a structure of infinite extent [4]. The second component of the gel structure, usually the solvent, must form a free-moving, continuous phase. The coherent network of real gels is responsible for the high stability against mechanical influences. The surrounding fluid enables the system to undergo infinitely large deformations. Gels are, therefore, characterized by ambivalent behavior: they

exhibit a unique combination of viscous and elastic properties. No structure, otherwise constituted, will sustain, without rupture, the high deformations typical for rubber-elastic materials. Macromolecules, inorganic polymers, like sulfur or polyphosphazenes, surfactants and biopolymers, such as proteins, elastin or collagen, display the previously mentioned characteristics. All these molecules are capable of building infinitely long, supermolecular network structures.

Cross-linked gel structures can be divided into different categories, depending on the nature and the strength of binding forces. There are at least two extreme cases which are often observed in colloidal systems: transient networks or permanent structures. When the cross-linking process is a result of chemical reactions, the structures are always of the permanent type, resulting in the formation of very stable junction points. These cross-linking points do not change during deformation processes and they confer elastic properties to the sample. Transient or temporary networks can be formed by physical contacts between the molecules. These might be hydrogen bonds, entanglements, van der Waals interactions, Coulomb forces or complex formations. In this case, the number of junction points may change during deformation processes. For longer times of mechanical loading, the molecules can undergo diffusional motions, which finally lead to an opening of junction points. These dynamic molecular rearrangements, referred to as relaxation phenomena, ultimately result in the external stresses decaying to zero. In the ideal case, the behavior of the system after a long time period is characteristic of a liquid. This phenomenon can be characterized by a limited value of the average lifetime of the junction points. At conditions where an experiment is short in comparison to the average lifetime, the number of cross-linking points remains constant. In this regime, the sample exhibits elastic properties. After long periods of loading times, however, all junction points may open and viscous flow results. The fundamental physical properties of these systems show a marked dependence on the duration of the measurement or on the frequency in dynamic rheological experiments. This type of behavior is well described by the expression "transient" or "temporary" network.

It is interesting to note that ultrathin films formed by adsorption of SPAN 65 molecules exhibit such viscoelastic features. Typical network properties can, hence, only be observed in certain time intervals. Here, we report the investigation of the basic rheological features of these films and also their basic molecular structure using Brewster-angle microscopy.

## Experimental

The surfactant SPAN 65 was obtained from Fluka. The high-pressure liquid chromatography diagram showed a large number of

different peaks, indicating a broad distribution of different chemical compounds. As it is very difficult to separate all these molecules, we used this surfactant mixture without further purification steps. As mentioned before, this detergent is frequently used in technical applications in order to stabilize foams or emulsions, and in all these samples it was also used as supplied. Being aware of the problem of working with technical grade surfactant mixtures, we examined the reproducibility of the rheological experiments, using different surfactant samples. The results were in pretty good agreement, with typical deviations of about 16%. As we will see that all relevant rheological data change by many orders of magnitude, these relatively small deviations can be neglected in comparison to the striking viscoelastic network response.

For measurements at the interface between dodecane and water, the surfactant was dissolved in desired amounts in the hydrophobic phase. Water was obtained from a pure water system (Seralpur PRO 90 CN). At the pure water surface, the surfactants were spread from a  $10^{-3}$  M solution in chloroform (p.a. Merck).

The shear rheological properties of flat membranes were determined in a Rheometrics fluid spectrometer (RFS II), which was equipped with a modified shear system [5]. The measuring cell consisted of a quartz dish (diameter 83.6 mm) and a thin biconical titanium plate (angle 2°, diameter 60 mm) which could be placed exactly at the interface between oil and water. The dish was first filled with the aqueous phase. The titanium plate was then positioned at the water surface and a solution of the surfactant was added. We measured the torque required to hold the plate stationary as the cylindrical dish was rotated with a sinusoidal angular frequency,  $\omega$ . In such experiments, the two-dimensional storage modulus,  $\mu'(\omega)$ , and the loss modulus,  $\mu''(\omega)$ , could be evaluated from the amplitude and phase angle of the stress and deformation signals.

At the water surface,  $\pi$ -A isotherms and Brewster-angle microscopy was performed with a BAM 2 from Nanofilm Technologie, Göttingen. The basic principles of Brewster-angle microscopy experiments are extensively described in Refs. [6, 7]. If a p-polarized light beam is incident at the Brewster angle to the surface of water (53.1°), no light is reflected. A video camera, arranged in the direction of the reflected light beam, will now observe darkness. In the presence of surface-active compounds, however, the refractive index of the water surface is slightly changed. As a consequence, the video camera will now obtain some light and the image of the network structure can be analyzed. Hence, one obtains a large optical contrast between the pure water surface (black regions) and those parts covered with surfactant molecules (white regions). It is interesting to note that the lateral resolution of the Brewster-angle microscope is related to the wavelengths of the incident laser beam (690 nm), and this technique allows the investigation of monomolecular films with a thickness of only 1 nm.

## Results

### Ultrathin networks at the dodecane–water interface

Even with the unaided eye it is possible to recognize the large viscous resistance of SPAN 65 films formed at the oil–water interface. This becomes evident by simple observing the diffusion process of small dust particles or air bubbles which are attached at the interface. More details concerning the rheological properties of these systems can be obtained from rate sweep experiments. In these tests, the stationary shear viscosity is measured as a function of the velocity gradient. Typical properties of these tests are summarized in Fig. 1.

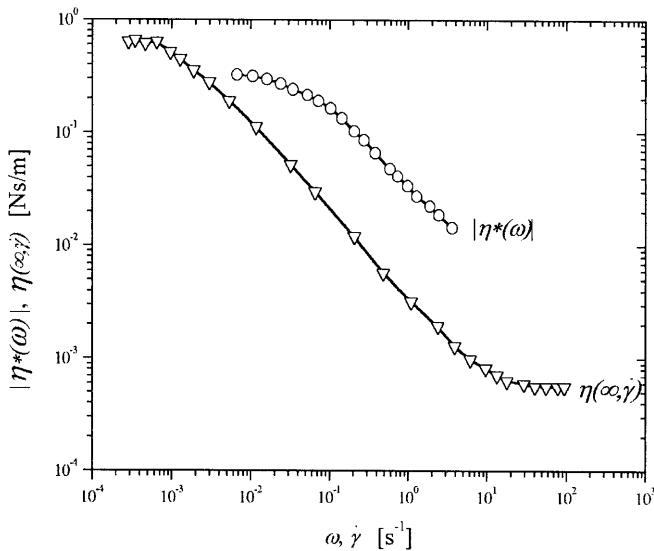


**Fig. 1** The steady-state shear viscosity and the magnitude of the complex viscosity as a function of the shear rate or the angular frequency for a SPAN 65 film at the interface between dodecane and water ( $c=0.5$  mmol/l,  $T=20$  °C)

In viscoelastic samples, all rheological properties are characterized by time-dependent material functions. If a step function shear rate is suddenly applied to the ultrathin network, one obtains an increasing shear stress, which finally reaches a plateau level. This regime of constant shear stress describes the steady-state values of the viscous resistance where the surfactant structure is in equilibrium with the external shearing force. Under these conditions, the supermolecular surfactant structures are aligned in the direction of flow or they are breaking owing to the action of shearing forces. The plateau value in the regime of very small shear rates is called the zero-shear viscosity,  $\eta(\infty,0)$ . This value describes the viscous resistance of the quiescent state of the network. In this regime the external shearing forces are so small that they cannot influence the surfactant film structure. In rheological experiments, this plateau is usually observed for  $\dot{\gamma}\lambda \ll 1$ . Here,  $\lambda$  denotes the relaxation time of the shear stress. With increasing amount of shear the viscosity decreases strongly and nonlinear phenomena occur. This typical behavior is called shear-thinning or pseudoplastic. The non-Newtonian behavior of these solutions is of great practical interest and is intimately connected with orientation processes or structural changes which occur during flow. When a suspension of rigid or semiflexible asymmetrical particles is subjected to a velocity gradient, a strong orientation results. Under the action of a velocity gradient, a particle will be oriented along the streamlines because in any other position its ends will be located in layers of different velocities, which exert an orientating force on the molecule. The strong alignment

of the anisometric particles is a typical dynamic process, because the suspended ellipsoids rotate in the fluid and do not rest in their position as observed in magnetic or electric fields. It is well known that in laminar flow, the anisotropic particles are forced to rotate with a nonuniform angular velocity. The Brownian motion, however, tends to counteract the hydrodynamic alignment by causing random fluctuations. The competition of both influences leads to the flow-induced decrease of the viscous resistance. It is also conceivable that the action of shear rates induces the rupture of supermolecular structures. In this case, for instance, a gel can be transformed into a sol state under the action of a velocity gradient. The completely oriented or destroyed structure is characterized by the lower plateau level, which is often called the second Newtonian plateau,  $\eta(\infty,8)$ . It is easy to recognize that this value is many orders of magnitude lower than the zero-shear viscosity.

Similar curves, as shown in Fig. 1, are often observed in solutions of entangled macromolecules which tend to form temporarily cross-linked networks in the quiescent state. For SPAN 65 monolayers the lengths of the paraffin chains are too short for the formation of entanglements, so we can exclude this special cross-linking mechanism. In analogy to these junction points it is, however, evident that the SPAN 65 films also form stable contacts points. The shear-induced deformation or structure breakup is completely reversible and on slowly decreasing the shear rate one obtains the same viscosity curve as measured before. All contacts between SPAN 65 molecules rapidly reform again in the quiescent state. This process can be characterized by relaxation times, which will be explained by the results of further experiments.

The viscoelastic properties of the sample are usually measured in periodic or dynamic experiments. In this case the shear strain is varied periodically with a sinusoidal alternation at an angular frequency,  $\omega$ . A periodic experiment at frequency  $\omega$  is qualitatively equivalent to a transient test at time  $t=1/\omega$ . In a general case, a sinusoidal shear strain is applied to the solution. The response of the liquid to the periodic change consists of a sinusoidal shear stress, which is out of phase with the strain. The shear stress is made up of two different components. The first component is in phase with the deformation and the second one is out of phase with the strain. From the phase angle,  $\delta$ , the amplitudes of the shear stress and the amplitude of the shear strain it is possible to calculate  $\mu'(\omega)$  and  $\mu''(\omega)$ .  $\mu'(\omega)$  describes the elastic properties of the sample and  $\mu''(\omega)$  is proportional to the energy dissipated as heat (viscous resistance). It is convenient to express the periodically varying functions as a complex quantity, which is termed the magnitude of the complex viscosity,  $|\eta^*(\omega)|$ . This quantity can be calculated from the following equation:

$$|\eta^*| = \frac{\sqrt{\mu'^2(\omega) + \mu''^2(\omega)}}{\omega} . \quad (1)$$

It can be shown that for most viscoelastic solutions there is a simple correlation between dynamic and steady-state flow characteristics [8]. In a first approximation the complex viscosity  $|\eta^*(\omega)|$  at a certain angular frequency  $\omega$  can be compared with the steady-state value of the shear viscosity  $\eta(\infty, \dot{\gamma})$  at the corresponding shear rate  $\dot{\gamma}$ . This famous correlation between linear viscoelastic functions and nonlinear effects is called the Cox–Merz rule [9].

$$|\eta^*(\omega)| = \eta(\infty, \dot{\gamma}) \quad \text{for } \omega = \dot{\gamma} \quad (2)$$

According to observations of Cox and Merz, both rheological functions coincide for entanglement networks of polymers [9]. Deviations, however, occur if other types of forces, such as hydrogen bonds, van der Waals or ionic interactions, contribute to the cross-linking process. The steady-state viscosity of these solutions is often much smaller than the corresponding dynamic values because the number of junction points is reduced during flow, whereas it remains stable in oscillatory experiments. For comparison purposes, we have also plotted the magnitude of the complex viscosity in Fig 1. It is easy to see that both viscosities do not coincide, and within the frequency or shear-rate interval investigated the magnitude of the complex viscosity is always larger than the shear resistance. This phenomenon can be explained by processes occurring during flow. We can, therefore, conclude that the contact points between the SPAN 65 molecules are different from entanglements, but they exhibit typical properties of temporary contacts, such as hydrogen bonds or van der Waals interactions.

The viscoelastic behavior of the ultrathin networks can be obtained from dynamic measurements. In this case the shear strain is varied periodically with a sinusoidal alternation at an angular frequency  $\omega$ . Relevant data of these experiments are summarized in Fig. 2.

The experimental curves exhibit typical properties of a generalized Maxwell material. In the regime of high frequencies, the two-dimensional storage modulus  $\mu'(\omega)$  attains a plateau value, and at these conditions the elastic response of the sample is dominant. It turns out, that  $\mu'(\omega) \gg \mu''(\omega)$  for  $\omega\lambda \gg 1$ . The plateau value describes the rubber-elastic properties of the sample. With decreasing angular frequency, the viscous properties become more important. In this regime, relaxation processes occur and the solution behaves as a liquid. The intersection point where  $\mu'(\omega) = \mu''(\omega)$  is characterized by an average value of the relaxation time. This constant can be calculated using the simple relation

$$\lambda = \frac{1}{\omega_{\text{int}}} . \quad (3)$$

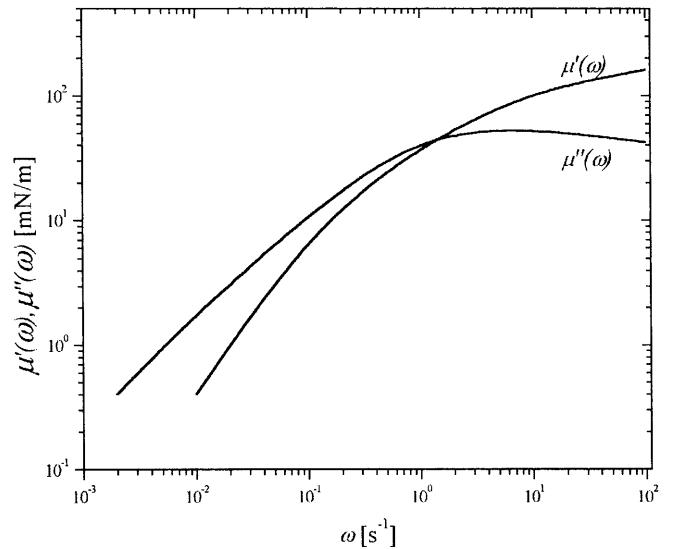


**Fig. 2** The two-dimensional storage and loss modulus as a function of the angular frequency for a SPAN 65 film formed at the interface between dodecane and water ( $c = 0.5 \text{ mmol/l}$ ,  $T = 20^\circ\text{C}$ )

This relaxation time describes the dynamic features of the ultrathin networks. In monolayers of surfactant molecules, stress decay can only occur by rupture processes of junction points. We can, therefore, conclude that the ultrathin SPAN 65 networks exhibit striking dynamic properties. These structures fluctuate and they are continuously built up and destroyed by the formation and breaking process of cross-linking points. In such systems the relaxation time describes an average lifetime or breaking time of the junction points. Under experimental conditions where the frequency is short in comparison to the reciprocal lifetime, a junction point cannot open during one oscillatory cycle. In this regime, the adsorbed layer behaves as a permanent cross-linked network. A completely different structure can be observed for small angular frequencies. In this regime, there are numerous breaking and reformation processes within the time scale of observation. As a consequence, an applied shear stress will completely relax and a fluidlike behavior results. The intermediate frequency range is characterized by an ambivalent behavior where both processes occur simultaneously. This regime is characterized by striking viscoelastic properties.

Additional information concerning the viscoelastic properties of the ultrathin films can be obtained from measurements of the relaxation modulus. In these transient experiments, a stepwise transition is used from one equilibrium state to another. Although the initial extension is infinitely fast, there is a certain time response of the viscoelastic sample, which can be measured to evaluate the desired rheological function. In relaxation experiments, a step-function shear strain,  $\gamma$ , is suddenly applied at  $t = 0$ . The resulting stress is

time-dependent, and this parameter is measured after deformation has occurred. From these data the relaxation modulus  $\mu(t)$  can be calculated:

$$\mu(t) = \frac{\sigma(t)}{\gamma_0} . \quad (4)$$

In the limit of small deformations (linear viscoelastic regime), the relaxation modulus does not depend on  $\gamma$  and it is only a function of time. From Eq. (4) it is clear that the relaxation modulus describes the shear-stress decay after the onset of shear strain. In samples of viscoelastic liquids an applied stress always relaxes to zero after infinitely long periods of time. Typical results for ultrathin SPAN 65 networks are summarized in Fig. 3.

A transient experiment, performed at time  $t$ , is qualitatively equivalent to a dynamic test performed at  $\omega = 1/t$ . That means both graphs  $\mu(t)$  and  $\mu'(\omega)$  are approximately mirror images reflected in the modulus axis. The exact relationship between these functions is given by the Fourier transformation.

$$\mu(t) = \frac{2}{\pi} \int_0^\infty \frac{\mu'(\omega)}{\omega} \sin \omega t \, d\omega . \quad (5)$$

This integral can be solved numerically or graphically if the starting function is known over a sufficiently wide range of frequency. It is easy to see that the two-dimensional relaxation modulus gives the same results as already mentioned for  $\mu'(\omega)$ . The dynamic features of the generalized Maxwell material can be characterized by a set of discrete relaxation times and relaxation moduli. Such a representation of experi-

mental values is called a discrete relaxation spectrum. Under conditions where many different relaxation times occur, it is convenient to use continuous spectra for the description of relaxation properties. Thus, an alternative expression for the relaxation modulus is given by [9]

$$\mu(t) = \int_{-\infty}^{+\infty} H(\lambda) \exp(-\frac{t}{\lambda}) d \ln \lambda . \quad (6)$$

It is often observed, that the relaxation spectrum,  $H(\lambda)$ , has a shape rather similar to  $\mu''(\omega)$  reflected in the modulus axis. The spectrum itself is not accessible by direct experiment. It is, however, possible to calculate it from measurements of  $\mu'(\omega)$ ,  $\mu''(\omega)$  or  $\mu(t)$  by numerical or graphical differentiation or by use of finite-difference methods. We shall not go into more details at this point. Typical results for the temporarily cross-linked SPAN 65 films are summarized in Fig. 4.

The maximum of  $H(\lambda)$  represents concentration zones of relaxation times. It is worthwhile mentioning that the extreme value at  $\lambda = 0.5$  s corresponds to the intersection point of  $\mu'(\omega)$  and  $\mu''(\omega)$  (see Fig. 2). The experimental values represented in Fig. 4 describe a broad distribution of different relaxation processes. This phenomenon is also observed in three-dimensional temporary networks. These structures have many possibilities to relax stress by different types of molecular motions.

It is interesting to note that similar dynamic relaxation processes are well known in aqueous three-dimensional viscoelastic solutions of wormlike micelles. In these systems, the shear-stress decay is attributed to

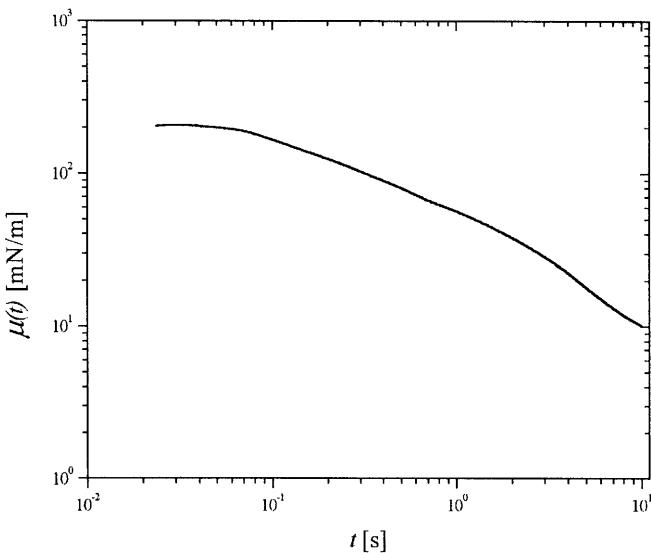


**Fig. 3** The two-dimensional relaxation modulus as a function of time for a SPAN 65 film formed at the interface between dodecane and water ( $c = 0.5$  mmol/l,  $T = 20$  °C)

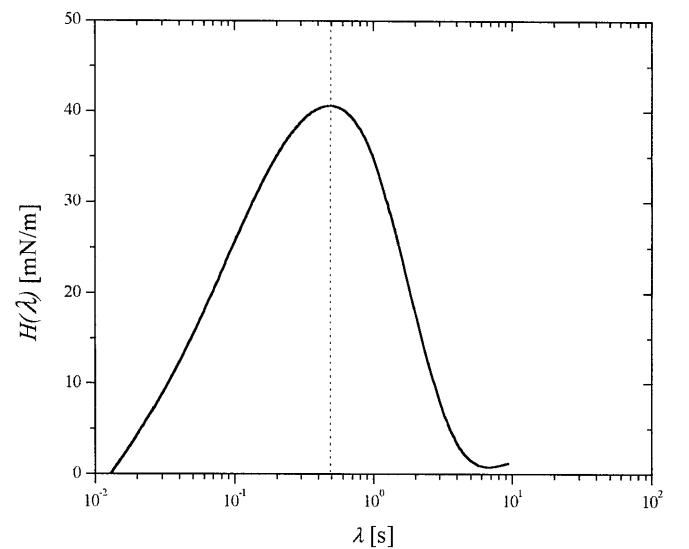


**Fig. 4** The relaxation spectrum as a function of the angular frequency for a SPAN 65 film formed at the interface between dodecane and water ( $c = 0.5$  mmol/l,  $T = 20$  °C)

the limited average lifetime of the anisometric aggregates. These phenomena are described by modified reptation theories, which were recently developed by Cates and coworkers [10–19].

### Ultrathin networks at the water surface

Dynamic networks of SPAN 65 can also be synthesized at the water-air surface. This is of great advantage because it allows simpler experiments to be used for the characterization of these structures. It is interesting to note that the general rheological behavior of these films does not change at the pure water surface. Relevant results concerning the viscoelastic properties are summarized in Fig. 5.

In these experiments, the film was spread from a  $10^{-3}$  M solution in chloroform. After evaporation of the solvent, the rheological properties were measured at a constant angular frequency until final plateau regimes of  $\mu'(\omega)$  and  $\mu''(\omega)$  were reached. Under these conditions, an intact network structure was formed and the dynamics features of these structures were evaluated from frequency-sweep experiments. Comparison with Fig. 2 reveals that the ultrathin networks, formed at the water surface, exhibit similar properties as at the dodecane–water interface. On close inspection, it becomes clear that the shape of the curves remains constant and that only the relaxation time and the plateau level of  $\mu'(\omega)$  are changed. This process is shown in Fig. 6.

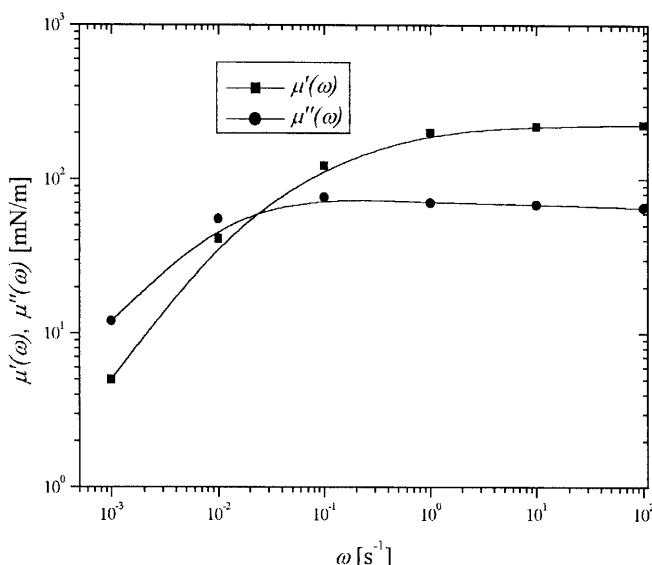


**Fig. 5** The two-dimensional storage and loss modulus as a function of the angular frequency for a SPAN 65 film formed at the water surface ( $\Gamma_m = 12$  molecules/nm $^2$ ,  $T = 20$  °C) and the water–dodecane interface (filled symbols;  $c = 0.5$  mmol/l,  $T = 20$  °C)

The behavior under harmonic oscillations of a Maxwell material can be described by [20]

$$\mu'(\omega) = \sum_{i=1}^n \mu'_{i,p} \cdot \frac{\omega^2 \lambda^2}{1 + \omega^2 \lambda^2}, \quad (7)$$

$$\mu''(\omega) = \sum_{i=1}^n \mu'_{i,p} \cdot \frac{\omega \lambda}{1 + \omega^2 \lambda^2}. \quad (8)$$

Here,  $\mu'_{i,p}$  denotes the plateau modulus of the two-dimensional shear modulus at high frequencies. It is evident that a master curve can be obtained by plotting  $\mu'(\omega)/\mu'_p$  and  $\mu''(\omega)/\mu'_p$  against  $\omega\lambda$ .  $\mu'_p$  describes the experimentally determined plateau value of  $\mu'(\omega)$ . Figure 6 shows unambiguously that the rheological data of the ultrathin SPAN 65 networks prepared at different interfaces do overlap. This means, at least, that the flow properties of these structures are very similar. For both types of membranes, we obtain the typical behavior of a generalized Maxwell material, showing the presence of temporarily cross-linked network structures.

Additional measurements concerning the viscoelastic properties can be obtained from strain-sweep experiments. In these dynamic tests, the deformation is varied at a constant angular velocity. Relevant results of these measurements are summarized in Fig. 7.

This experiment measures the stability of the membrane and indicates the critical deformation initiating film rupture. It is worth mentioning that a linear stress-strain relationship is only observed at deformations below 0.1%. Such small values are typical for energy-

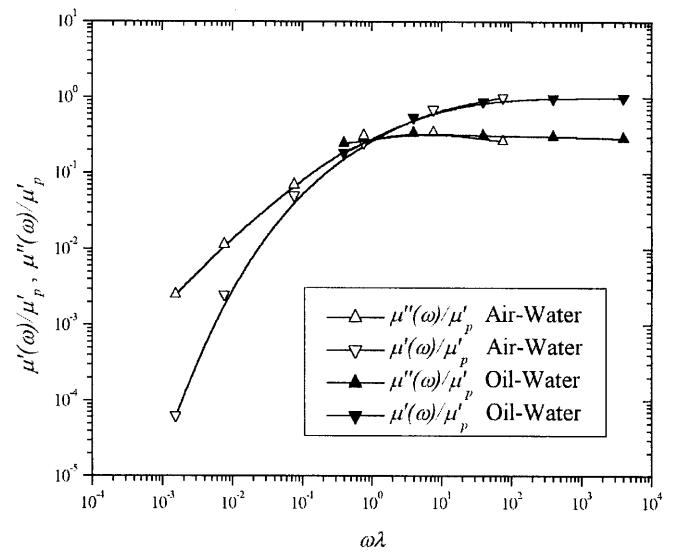


**Fig. 6** The normalized two-dimensional storage and loss modulus as a function of the angular frequency for a SPAN 65 film formed at the water surface (open symbols;  $\Gamma_m = 12$  molecules/nm $^2$ ,  $T = 20$  °C) and the water–dodecane interface (filled symbols;  $c = 0.5$  mmol/l,  $T = 20$  °C)

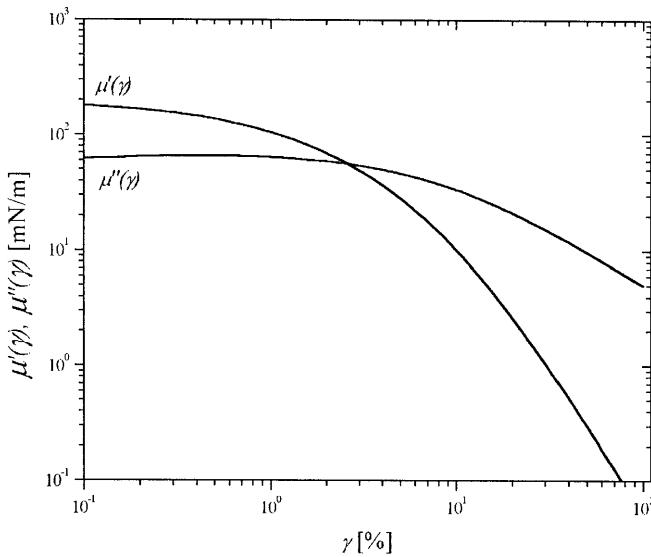


**Fig. 7** The two-dimensional storage and loss modulus as a function of the deformation angular frequency for a SPAN 65 film formed at the water surface ( $\Gamma_m = 12 \text{ molecules/nm}^2$ ,  $T = 20^\circ\text{C}$ ,  $\omega = 0.1 \text{ s}^{-1}$ )

elastic systems. Ideal rubberlike materials have much larger threshold values of about 100–500% [21]. On a molecular scale, the nonlinear regime is due to reversible structure breakdown and recovery after removal of stress. In viscoelastic ultrathin membranes, linear properties are always observed if  $\hat{\gamma}\omega\lambda \ll 1$ . Here,  $\hat{\gamma}$  denotes the amplitude of the shear strain. Under these experimental conditions, shear flow does not affect the surfactant structure and the system is still in the quiescent state. The small regime of linear viscoelastic properties points to the existence of energy-elastic properties, which are typical for hydrogen bonds or complex formations. In this case, there is a well-defined distance between the cross-linked molecules, and the application of external forces leads to rupture and breaking processes. For the ultrathin networks of SPAN 65, the quiescent gel state is then transformed into a sol state.

At the water surface, it is easy to investigate the concentration dependence of the rheological properties. Typical results of these experiments are summarized in Fig. 8.

In the highly dilute surface concentration regime, the plateau value rapidly increases. The theory of rubberlike elasticity predicts [21]

$$\mu'_p = A\Gamma_{\text{el}} kT . \quad (9)$$

In this equation,  $A$  denotes a front factor, which is very often of the order of 1.  $\Gamma_{\text{el}}$  describes the number of elastically effective chains per unit area. Comparing Eq (9) with Fig. 8 leads to the results, that  $\Gamma_{\text{el}} \approx 16\Gamma_m$ . The assumption that each free electron pair of an oxygen

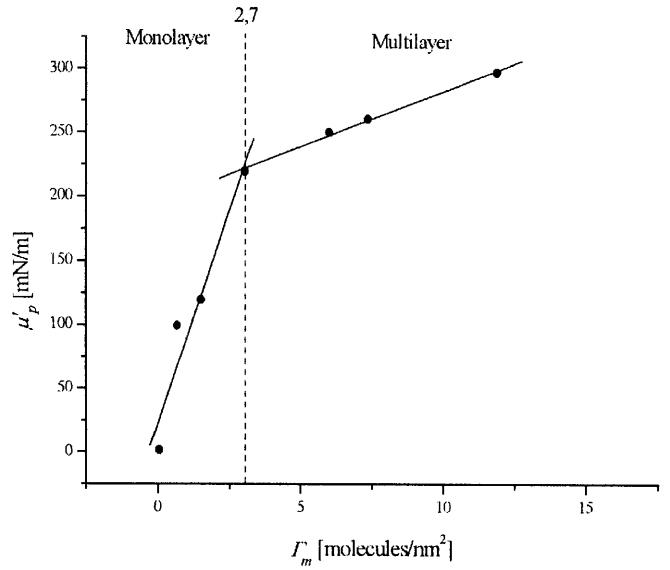


**Fig. 8** Plateau value of the two-dimensional storage modulus as a function of the surface concentration  $\Gamma_m$  for ultrathin networks of SPAN 65 at  $T = 20^\circ\text{C}$

atom in SPAN 65 can just form one hydrogen bond also leads to an average number of 16 possible junctions to neighboring molecules. On the basis of this simple argument, the measured cross-linking functionality of 16 seems to be realistic and this value explains the striking viscoelastic properties of these ultrathin networks.

At a surface concentration of about 2.7 molecules/ $\text{nm}^2$ , Fig. 8 shows a breaking point where different properties result. This phenomenon coincides very well with the threshold concentration, where we observe multilayers in images of “Brewster-angle microscopy” (see Fig. 11). We can, therefore, conclude that this point describes the transition from monolayers to multilayers. It is interesting to note that the frequency dependence of  $\mu'(\omega)$  and  $\mu''(\omega)$  does not change in the multilayer concentration regime.

Besides the zero-shear modulus,  $\mu'_p$ , there are other rheological constants, such as the relaxation time, which change in the vicinity of saturated monolayers (Fig. 9). On close inspection, there is also a small breaking point where the double layer should be transformed into the multilayer ( $\Gamma_m \approx 3 \text{ molecules/nm}^2$ ).

These results point to the existence of well-defined surfactant structures at the water surface.

#### Brewster-angle microscopy of SPAN 65 films observed at the water surface

The phase diagram of insoluble surfactant films can be evaluated from the  $\pi$ - $A$  isotherm (Fig. 13). Typical results of these measurements are summarized in

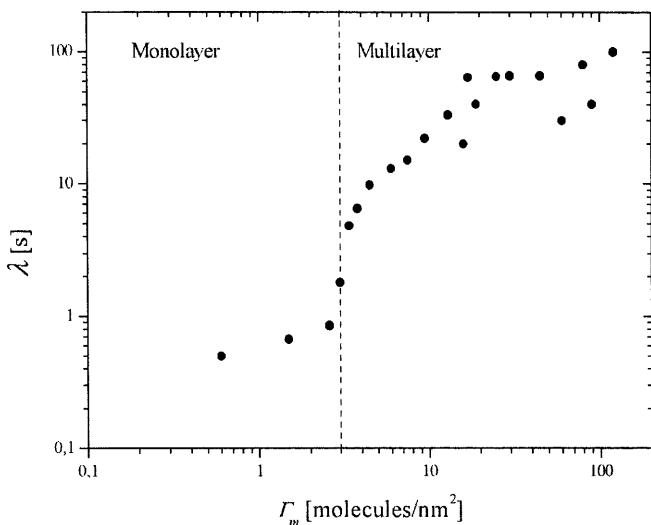


**Fig. 9** The average relaxation modulus as a function of the surface concentration for ultrathin networks of SPAN 65 at  $T=20\text{ }^{\circ}\text{C}$

Fig. 10. Arrows indicate characteristic features in the diagram. Corresponding Brewster-angle microscope images are shown in Fig. 11.

The isotherm shows the typical pattern of a condensed film. The classification into gaseous-, solid- and liquid-analogous phases used is inapplicable for these films because the surfactant monolayer consists of a mixture of different sugar esters. The characterization took place on the basis of the different experiments we performed in order to compensate the heterogeneity of

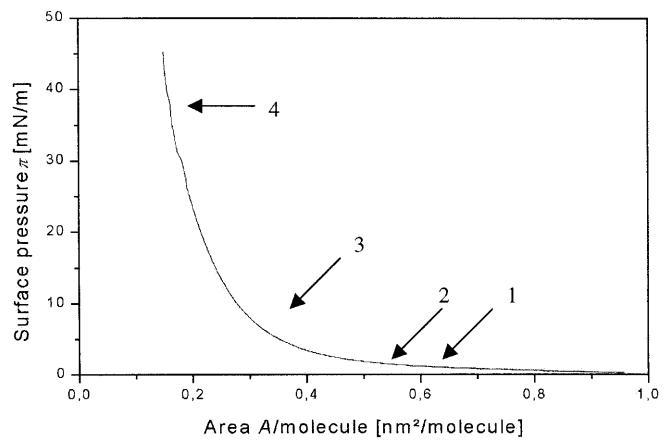
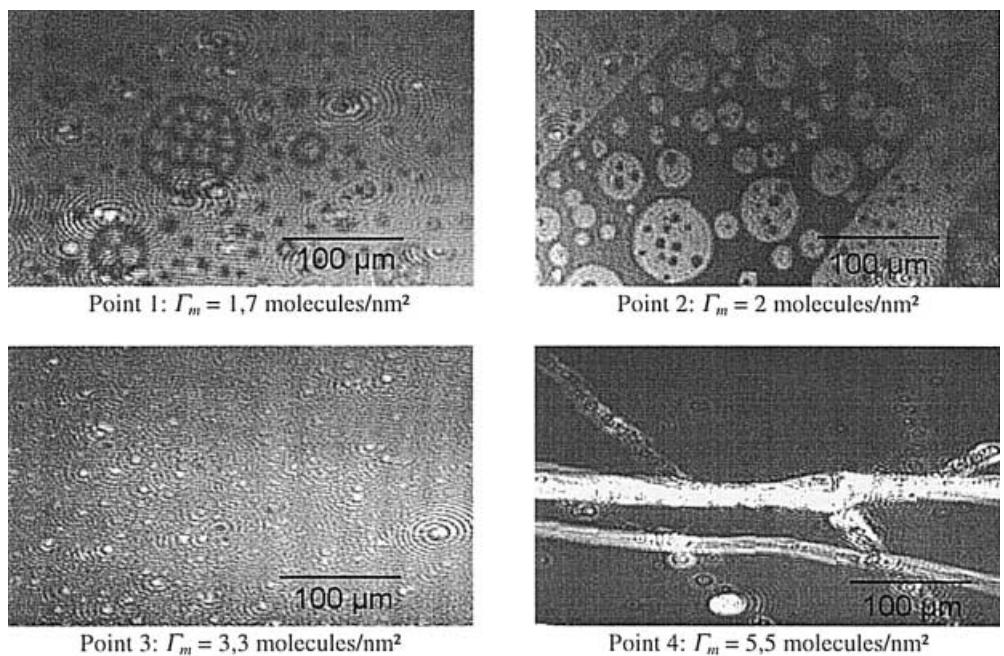


**Fig. 10** Surface pressure-area ( $\pi$ -A) isotherm for SPAN 65 at  $T=20\text{ }^{\circ}\text{C}$

the film. For small values of  $\pi$  the film is still in a gas-analogous state (1), then it changes into a liquid-analogous phase (2). At  $\pi=28\text{ mN/m}$  a change in the slope of the isotherm is observed and at higher surface pressures the film is in a solid-analogous state. Under these conditions the structure is density packed, corresponding to a disordered solid. If compression increases the film collapses (4).

The images of the four marked points are shown in Fig. 11. The picture sequence describes the change in the film with increasing surface concentration,  $\Gamma_m$ . At the beginning of film formation a heterogeneous structure was observed, characterized by disklike clusters with

**Fig. 11** Brewster-angle microscope images of SPAN 65



defects. The dark areas between the clusters represent the uncovered water surface. On the other hand, areas are detectable (point 1) where the film is densely packed (see lower image field). At surface concentrations of 2 molecules/nm<sup>2</sup> the free water surface decreases. At these conditions the SPAN 65 film is nearly closed, but it still contains some holes of spherical geometry. At surface concentrations of 3.3 molecules/nm<sup>2</sup> one observes a homogenous, densely packed film. Bright points indicate dust particles. At the collapse the film breaks and multilayers are formed. This is recognized by bright strips at surface concentrations of about 5.5 molecules/nm<sup>2</sup>.

During the relaxation of the film an interesting phenomenon can be observed: starting from a surface concentration of  $\Gamma_m < 3$  molecules/nm<sup>2</sup> the film tears off. A different structure which corresponds to a two-dimensional foam is formed. With decreasing concentration

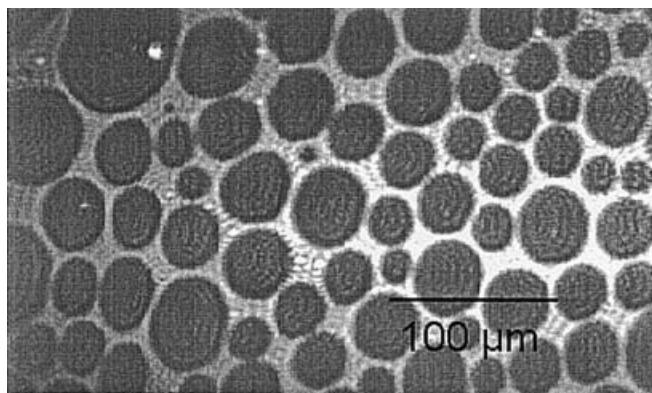


**Fig. 12** Foam structure of SPAN 65 at expansion;  $\Gamma_m = 1.5$  molecules/nm<sup>2</sup>

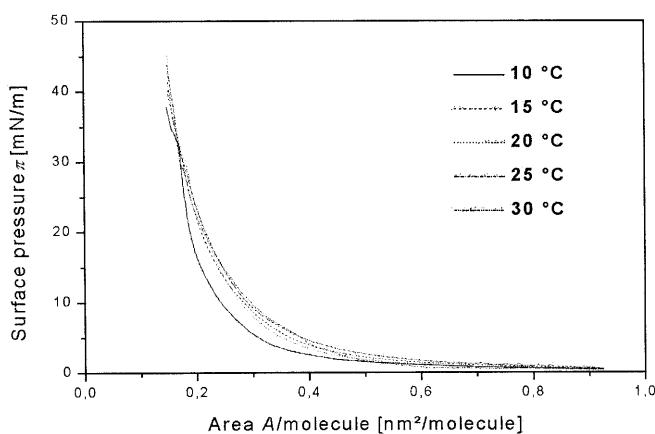


**Fig. 13**  $\pi-A$  isotherms of SPAN 65 at different temperatures

the uncovered areas become larger. A characteristic picture of this foam structure is represented in Fig. 12.

The phase diagrams of SPAN 65 in a temperature range of 10–30 °C are shown in Fig. 13.

One can recognize that variation of temperature does not significantly influence the distribution of the isotherm. At the beginning of compression there is only a weak slope of surface pressure, then the slope increases. The inflection point of the solid-analogous state shifts to smaller values if the temperature increases. This is significant for increasing dynamic motions of the molecules.

## Conclusions

In the preceding sections we have seen that the self-association process of SPAN 65 surfactants leads to the formation of dynamic networks at different types of fluid interfaces. The cross-linking process of this structure only becomes evident in the regime of short time scales. If an experiment is performed at  $t \ll \lambda$  an intact network structure is observed. If, on the other hand, the observation time is very long compared to the average relaxation time, we mainly detect fluid like response. The intermediate frequency or time range is characterized by striking viscoelastic properties. Such network like features can only result if strong, attractive interactions between the surfactant molecules lead to two-dimensional self-association processes. The experimental data of the concentration dependence of the surface-shear modulus suggest that hydrogen bonds may be responsible for this special behavior. This seems, however, not to be the only source of cross-linking processes because the surfactant SPAN 60, a similar compound, does not show the formation of these supermolecular structures. The difference between these surface-active molecules is mainly given by the number of paraffin chains: SPAN 65 has an average value of 3 and SPAN 60 only 1 of these hydrophobic chains. As it is well known that long paraffin chains also interact by van der Waals attractions, there might also be a combination of hydrogen bonds and hydrophobic forces, which finally leads to the observed dynamic cross-linking process.

It is worthwhile mentioning that the ultrathin SPAN 65 networks exhibit interesting rheological properties. They can, therefore, be used to form stable emulsions, foams or microcapsules. This might be interesting for a large number of new technical applications.

**Acknowledgements** Financial support by grants of the Deutsche Forschungsgemeinschaft (SFB 1690), the University of Essen (Fachbezogene Arbeitsgruppe) and the Fonds der Chemischen Industrie are gratefully acknowledged.

## References

1. Achenbach B, Husmann M, Rehage H (2000) In: Blass E (ed) Transport mechanisms across fluid interfaces. VCH, Weinheim, p 136
2. Edwards DA, Brenner H, Wasan DT (1991) Interfacial transport processes and rheology. Butterworth-Heinemann, Boston
3. Malhotra AK, Wasan DT (1988) In: Ivanov IB (ed) Thin liquid films. New York, p 829
4. Stauffer DAA (1995) Perkolationstheorie – Eine Einführung. VCH, Weinheim
5. Pieper G, Rehage H, Barthès-Biesel D (1998) J Colloid Interface Sci 202:293
6. Hönig D, Möbius D (1991) J Phys Chem 95:4590
7. Hénon S, Meunier J (1991) Rev Sci Instrum 62:936
8. Cox WP, Merz EH (1958) J Polym Sci 28:619
9. Kulicke WM (1986) Fließverhalten von Stoffen und Stoffgemischen. Basel
10. Cates ME (1987) Macromolecules 20:2289
11. Cates ME (1988) J Phys (Paris) 49:1593
12. Cates ME, Safran SA (1997) Curr Opin Colloid Interface Sci 2:359
13. Grand C, Arrault J, Cates ME (1997) J Phys II 7:1071
14. Cates ME (1996) J Phys Condens Matter 8:9167
15. Cates ME, Safran SA (1996) Curr Opin Colloid Interface Sci 1:327
16. Callaghan PT, Cates ME, Rofe CJ, Smeulders JBAF (1996) J Phys II 6:375
17. Spenley NA, Cates ME, Mcleish TCB (1993) Phys Rev Lett 71:939
18. Turner MS, Marques C, Cates ME (1993) Langmuir 9:695
19. Marques CM, Turner MS, Cates ME (1994) J Non-Cryst Solids 172:1168
20. Tschoegl NW (1989) The phenomenological theory of linear viscoelastic behavior: an introduction. Springer, Berlin Heidelberg New York
21. Ferry JD (1980) Viscoelastic properties of polymers. Wiley, New York